



OPEN ACCESS

EDITED BY

Tadeusz Hryniewicz,
Koszalin University of Technology, Poland

REVIEWED BY

Sathish Kumar Palaniappan,
King Mongkut's University of Technology
North Bangkok, Thailand
Vasudevan Mangottiri,
Bannari Amman Institute of Technology
(BIT), India

*CORRESPONDENCE

Nian Qi,
✉ Qi_nian529@126.com

RECEIVED 23 November 2025

REVISED 30 January 2026

ACCEPTED 02 February 2026

PUBLISHED 20 February 2026

CITATION

Shen S, Zhang W and Qi N (2026)
Experimental study on chemical compatibility
of polymer amended bentonite subjected to
inorganic salt solutions.
Front. Mater. 13:1752439.
doi: 10.3389/fmats.2026.1752439

COPYRIGHT

© 2026 Shen, Zhang and Qi. This is an
open-access article distributed under the
terms of the [Creative Commons Attribution
License \(CC BY\)](https://creativecommons.org/licenses/by/4.0/). The use, distribution or
reproduction in other forums is permitted,
provided the original author(s) and the
copyright owner(s) are credited and that the
original publication in this journal is cited, in
accordance with accepted academic practice.
No use, distribution or reproduction is
permitted which does not comply with
these terms.

Experimental study on chemical compatibility of polymer amended bentonite subjected to inorganic salt solutions

Shengqiang Shen, Wenbin Zhang and Nian Qi*

School of Civil Engineering and Architecture, Nanjing Vocational Institute of Transport Technology, Nanjing, China

This study aims to improve the chemical stability and engineering performance of bentonite slurry used in slurry trench cutoff walls, which often suffers from reduced swelling and permeability when exposed to saline environments. To address this, five superabsorbent polymers-polyanionic cellulose (PAC), hydroxypropyl methylcellulose (HPMC), carboxymethyl starch sodium (CMS), xanthan gum (XG), and sodium polyacrylamide (Na-PAM), were evaluated as additives to enhance unamended bentonite (CB). Key performance indicators including swell index, Marsh viscosity, filtrate loss, and hydraulic conductivity were systematically measured in CaCl_2 solutions (0–100 mM). Results show that XG-amended bentonite (XB) significantly outperforms CB, achieving higher swell index (24.2 vs. 15.9 mL/2 g) and liquid limit (403% vs. 267%), while maintaining low filtrate loss and acceptable viscosity under saline conditions. Hydraulic conductivity tests indicate a 75.3% reduction in permeability for XB filter cakes compared to CB. Additionally, polymer performance varies with cation type, with Pb^{2+} causing more severe degradation than Ca^{2+} due to pH effects. The study demonstrates that polymer amendments, particularly XG, can effectively enhance bentonite performance in saline environments, providing practical guidance for the design and construction of durable slurry trench cutoff walls.

KEYWORDS

chemical compatibility, hydraulic conductivity, polymer-amended bentonite, slurry trench walls, xanthan gum

1 Introduction

Environmental protection and groundwater management are critical concerns in modern construction, particularly in contaminated sites where the risk of hazardous materials leaching into surrounding ecosystems is high (de Carvalho Balaban et al., 2015; Balaganesh et al., 2023). One common solution to mitigate this risk is the use of slurry trench cutoff walls, which are designed to control the movement of contaminated groundwater (Sharma and Reddy, 2004; Wu et al., 2020). Traditionally, various materials and methods have been employed for these barriers, with bentonite slurry emerging as one of the most effective options due to its ability to form a low-permeability barrier (Philip, 2001; Opdyke and Evans, 2005; Li et al., 2015; Li et al., 2017). However, past and current practices in slurry trench construction face significant challenges, including issues related to the stability of the slurry during installation, long-term performance under varying environmental conditions, and the cost-effectiveness of the materials involved

(Tong et al., 2022; Evans et al., 2024). These challenges have led engineers to continually seek improvements in the formulation of the slurry and the methods of application. Bentonite slurry is widely used in constructing these cutoff walls, particularly because it stabilizes trench walls during excavation and creates a uniform barrier with low hydraulic conductivity ($<10^{-9}$ m/s) through self-weight consolidation (Ryan et al., 2022). This barrier effectively restricts the migration of contaminants by blocking pathways for groundwater flow. However, despite its extensive application, the performance of bentonite slurry, both during construction and over time, remains a central concern for engineers, particularly because it plays a crucial role in environmental containment. Understanding its long-term performance under changing environmental conditions, including exposure to saline or high-ionic-strength solutions, is critical for ensuring the durability and effectiveness of slurry trench cutoff walls (Ashmawy et al., 2002; Di Maio, 1996; Rout and Singh, 2020; Jia-Kai et al., 2023).

The primary functions of bentonite slurry in slurry trench cutoff walls include: (1) the formation of a filter cake less than 3 mm thick that traps fine bentonite particles within the pore spaces of native soils, creating a low-permeability barrier ($<10^{-12}$ – 10^{-9} m/s) that prevents fluid movement; and (2) providing lateral hydraulic resistance to maintain trench wall stability during excavation (Li et al., 2021a; Evans et al., 2024; Evans and Ruffing, 2025). To ensure proper construction and long-term functionality, the slurry must possess specific rheological properties, such as Marsh viscosity (40–45 s), filtrate loss (<25 mL), pH (6.5–10.0), and density (1.05–1.10 g/cm³), as outlined in ASTM D5891 and API RP13B-1 standards (Du et al., 2021). These properties guarantee the formation of stable filter cakes and ensure the uniformity of backfills, both of which are essential for maintaining barrier integrity over time.

Despite the widespread use of bentonite slurry in environmental containment, challenges remain regarding its long-term performance in the face of changing environmental conditions. Research has shown that bentonite filter cakes exhibit low hydraulic conductivity in tap water, as measured by the modified fluid loss test (MFL) (Du et al., 2021). However, when exposed to concentrated ionic solutions (e.g., >300 mM), the hydraulic conductivity of bentonite increases significantly, more than tenfold compared to tap water (Liu et al., 2016; Setz et al., 2017). This presents a significant challenge, as bentonite's hydraulic properties can deteriorate in real-world conditions where contaminants often have high ionic strength. Current research has focused on modifying bentonite with various additives to enhance its chemical compatibility and maintain its low hydraulic conductivity even in concentrated solutions. To address these challenges, polymers have emerged as an effective solution (Di Emidio et al., 2015; Pandey et al., 2019; Li et al., 2021b; Fu et al., 2023; Syed Masoodhu et al., 2024; Masoodhu et al., 2025). Polymers such as carboxymethyl cellulose (CMC), sodium polyacrylate, and xanthan gum are increasingly used to modify the properties of bentonite in saline or high-ionic-strength environments. These polymers enhance the swelling behavior of bentonite by providing additional stability to the clay structure, even when exposed to ionic solutions. The presence of polymers helps to maintain the bentonite's capacity to form a stable filter cake and reduce permeability in saline environments (Tian et al., 2019). For example, polymers like CMC can increase the viscosity of the slurry, helping it to resist the dispersion of bentonite

particles in saline solutions and maintain the required structural integrity during the construction process. These modifications have shown promise in improving the hydraulic performance of bentonite in contaminated environments. However, the literature reveals that existing polymer-modified bentonites often lack comprehensive studies on their long-term hydraulic performance and chemical stability in highly contaminated solutions, such as those containing calcium chloride (CaCl₂) and lead nitrate [Pb(NO₃)₂]. Moreover, many studies have focused on individual polymer types without direct comparisons, leaving a gap in our understanding of which polymer(s) provide the most durable and effective enhancements to bentonite slurry (Mazzieri et al., 2017).

This study aims to address these gaps by evaluating the fundamental properties and hydraulic performance of polymer-enhanced bentonite filter cakes, specifically in the presence of calcium chloride (CaCl₂) solutions. We selected five commonly used industry-standard polymers—Hydroxypropyl Methylcellulose (HPMC), Sodium Polyacrylate (Na-PAM), Polyanionic Cellulose (PAC), Carboxymethyl Starch (CMS), and Xanthan Gum (XG), which are known to improve the chemical compatibility of bentonite in aqueous solutions. The primary objective is to assess the effect of these polymers on bentonite's swelling capacity, specific gravity, liquid limit, and hydraulic conductivity under conditions simulating contaminated environments. Among the polymers tested, xanthan gum (XG) was identified as the most promising additive, and subsequent investigations will focus on its impact on the long-term performance of bentonite filter cakes. Specifically, this study will evaluate the construction workability of xanthan gum-modified bentonite slurry, the hydraulic conductivity of modified filter cakes in contaminated liquid environments, and the chemical compatibility of the filter cakes when exposed to CaCl₂ and Pb(NO₃)₂ solutions. By providing a comprehensive comparison of polymer-modified bentonites, this research aims to establish the most effective modification strategies for enhancing the durability and performance of bentonite slurry in environmental containment applications.

2 Materials and methods

2.1 Materials

2.1.1 Constituent soils and polymer

The unamended bentonite (i.e., Calcium-based bentonite, CB) used in the experiments is a commercial-grade sodium bentonite sourced from Zhenjiang, Jiangsu Province. The selection of CB tested here is mainly to its wide distribution and easy availability in China as compared to the Sodium-based bentonite (NB). Although NB possesses superior engineering performance in slurry wall construction, it has limited stock in China and is relatively expensive. The fundamental physical properties are presented in Table 1, and the particle size distribution curve illustrated in Figure 1. The grain size fractions <75 μ m and <2 μ m accounted for 100% and 32.5%, respectively. The liquid limit (w_L), plastic limit (w_P), and plasticity index (IP) were determined to be 272.3%, 34.2%, and 233.5%, respectively. The index properties of polymers provided by the manufacturer are summarized in Table 2. The ion types of polymers include anionic and nonionic types. The average molecular weight

TABLE 1 Basic engineering properties of tested bentonite.

Physical indicators	Value	Test method
Soil classification	CH	ASTM D2487
Fine content, %	100	ASTM D422
Clay content, %	69	ASTM D422
Specific gravity (G_s)	2.72	ASTM D854
Liquid limit (w_L)	269.4	ASTM D4318
Plastic limit (w_p)	34.2	ASTM D4318
pH	10.33	ASTM D4972
SSA (m^2/g)	252	ASTM D1993-22
CEC (meq/100 g)	48.1	ASTM D7503

SSA, is specific surface area; CEC, is cation exchange capacity; CH, is high liquid limit clay; ASTM, is American Society for Testing and Materials.

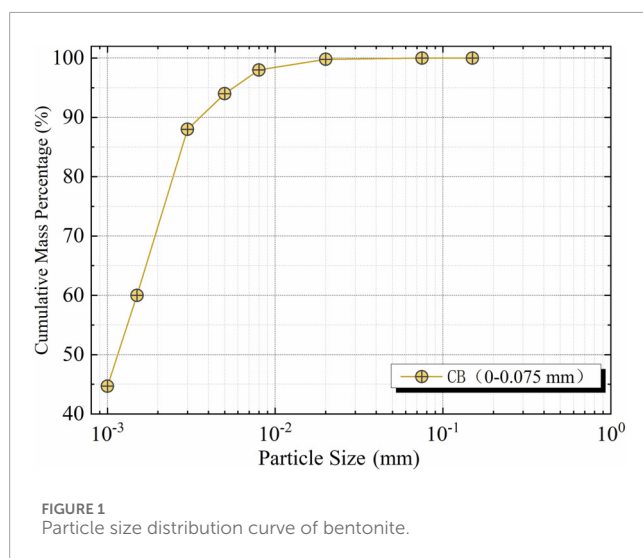


FIGURE 1 Particle size distribution curve of bentonite.

of all polymers is equal to or greater than 800,000, and the specific gravity of the polymers is less than 1.32, which is lower than that of soil minerals.

2.1.2 Test liquids

Calcium chloride ($CaCl_2$) solution was used as the simulated contaminated groundwater. The $CaCl_2$ concentrations were set at 5, 20, 50, and 100 mM, corresponding to Ca^{2+} mass concentrations ranging from 0 to 2,400 mg/L. This range aligns with the groundwater pollutant levels reported in previous literature (Du et al., 2021; Malusis and McKeehan, 2013). Deionized water (DW) served as the control group. The index properties of DW and $CaCl_2$ solutions are summarized in Table 3. Triplicate samples were tested for determining these five property indexes presented in this table, and thus, a total of 75 trials were made in these tests.

2.2 Test method

2.2.1 Polymer optimal selection test

A preliminary experiment was conducted to rapidly identify suitable polymers for modifying bentonite. Five polymer-amended bentonites were prepared by mixing dried bentonite with 2% polymer (by dry weight of CB). The mixtures were poured into hermetically sealed polyethylene bottles and vigorously shaken with an overhead stirrer for 1 h at a speed of 60 r/min and a controlled temperature of $20\text{ }^\circ\text{C} \pm 2\text{ }^\circ\text{C}$. To assess improvements in the constructability of polymer-amended bentonite, slurries were made by blending the polymer-amended bentonite with liquid (tap water or $CaCl_2$ solution) using a high-speed stirrer for 5 min. The slurries were then stored in plastic bottles for 24 h to hydrate. The engineering properties, including density, marsh funnel viscosity, filtrate volume, and pH, of the bentonite slurries were measured in accordance with API 13B-1 (API, 2009). Target values for the slurry were based on guidelines from USEPA (1984) and USACE (2010). The target values for slurry workability can be found in Table 7 of the following Section 3.2.2.

2.2.2 Engineering properties test

After thoroughly evaluating the swell index, engineering properties in saline conditions, and hydraulic performance of the bentonite filter cake, xanthan gum was selected as the amendment for further study of polymer-amended bentonite. The preparation process for the Xanthan gum-amended bentonite (XB) mixture followed the method previously described. The polymer dosage varied from 0% to 4% by weight of dry bentonite, as determined by Equation 1. The bentonite dosage (CB), representing the ratio of dry bentonite mass to total slurry mass, ranged from 6% to 10%, calculated via Equation 2. The mass of slurry can be calculated as the following Equation 3. Table 4 outlines the experimental design used to analyze the slurry properties of the amended bentonite.

$$C_p = \frac{m_p}{m_s} \times 100\% \quad (1)$$

$$C_B = \frac{m_s}{m_{\text{slurry}}} \times 100\% \quad (2)$$

$$m_{\text{slurry}} = m_s + m_p + m_w \quad (3)$$

where C_p is Polymer dosage (%), C_B is bentonite dosage (%), m_p is Polymer mass (g), m_s is dry bentonite mass (g), m_w is the mixing water, and m_{slurry} is the total slurry mass (g).

2.2.3 Modified filtrate loss (MFL) test

Before performing the modified filtrate loss test, the slurries were stirred for an extra 2 min. The tests used the API standard filtration apparatus with a 76.2-mm inner diameter, following ASTM D5891 (Chung and Daniel, 2008; Liu et al., 2014; Shen and Wei, 2018). Figure 2 shows the schematic diagram of the modified filtrate loss test. The filtrate volume was recorded within 5 min, while the entire experiment lasted 30 min. As shown in Table 3, the concentrations of $CaCl_2$ were established at 5, 20, 50, and 100 mM, with tap water (i.e., 0 mM) serving as a control for all samples. Experiments were performed under an applied air pressure of 100 kPa. Following the completion of the test, the thickness of the filter cakes (L) was measured on two occasions utilising a vernier calliper, and

TABLE 2 Index properties of the polymers.

Polymers	Molecular weight, Da	Apparent viscosity, mPa·s	Substitution degree	Specific gravity, G_s	Chemical formula
PAC	1,730,000	35	1.4	1.26	$[C_6H_7O_2(OH)_2CH_2COONa]_n$
HPMC	585,000	1,500	3.4	1.31	$(C_{10}H_{18}O_6)_n$
CMS	800,000	150	0.6	1.26	$[C_6H_7O_2(OH)_2OCH_2COONa]_n$
XG	2,510,000	1,600	1.26	1.24	$(C_{35}H_{49}O_{29})_n$
K-PAM	1,250,000	1,300	0.8	1.32	$(C_3H_6O_2)_n(C_3H_5KO_2)_m$

TABLE 3 Index properties of CaCl₂ solution used in tests.

Designed concentrations (mM)	Measured concentration (mg/L)	Specific gravity	Absolute viscosity/ μ (mPa·s)	Electric conductivity (μ S/cm)	pH
DW	0	1.00	1.04	0.01	6.52
5	207	1.00	1.04	752	6.25
20	828	1.01	1.05	2,728	6.45
50	2022	1.02	1.06	7,835	6.55
100	19,525	1.02	1.08	16,907	6.72

TABLE 4 Properties of polymer-amended bentonite and slurries.

Test content	Sample type	Bentonite mass ratio (%)	Polymer dosage (% by dry weight with bentonite)	Water mass ratio (%)
(1) Specific gravity (2) Swell index	CB	100	0	—
	XB	96, 98, 99, 99.5	0.5, 1, 2, 4	—
Slurry workability	CB slurry	6, 8,10	0	90, 92, 94
	XB slurry	6, 8,10	0.5, 1, 2, 4	90, 92, 94

the mean values were documented. Subsequently, the filter cakes were meticulously separated from the filter paper to evaluate their water content. This study calculated and reported the average void ratio. The hydraulic conductivity (k) of the bentonite filter cake was measured using the following equation (Chung and Daniel, 2008; Liu et al., 2014; Shen and Wei, 2018):

$$k_c = \frac{\beta \gamma_w V_t^2}{2P_0 A^2 t} = \frac{\beta \gamma_w}{2A^2 \varphi} \tag{4}$$

where γ_w is the unit weight of the chemical solution (kN/m³), V_t is the filtrate volume at time t (mL), and P_0 denotes the total applied pressure, which corresponds to the air pressure used in this study (kPa); A represents the cross-sectional area of the bentonite filter cake (cm²); φ is the slope of the $P_0 V_t/t - V_t$ relation curve

(kPas/cm⁶); and β is determined using the following Equation 5 (Chung and Daniel, 2008; Liu et al., 2014; Shen and Wei, 2018):

$$\beta = \frac{BC \rho_L (1 + e_{ave})}{(1 - BC) \rho_s - e_{ave} BC \rho_L} \tag{5}$$

where BC indicates the bentonite dosage of the slurry (%); ρ_L and ρ_s represent the densities of the solution and bentonite (g/cm³), respectively; and e_{ave} is the average void ratio of the bentonite filter cake.

At the end of the MFL test, a thin layer of a jelly-like bentonite-chemical mixture atop the bentonite filter cake was carefully and quickly removed with filter papers. The filter cake was then placed in an aluminum container for water content analysis. After oven drying, the bentonite was ground into a fine powder to determine its specific gravity according to ASTM D854. The average void ratio was

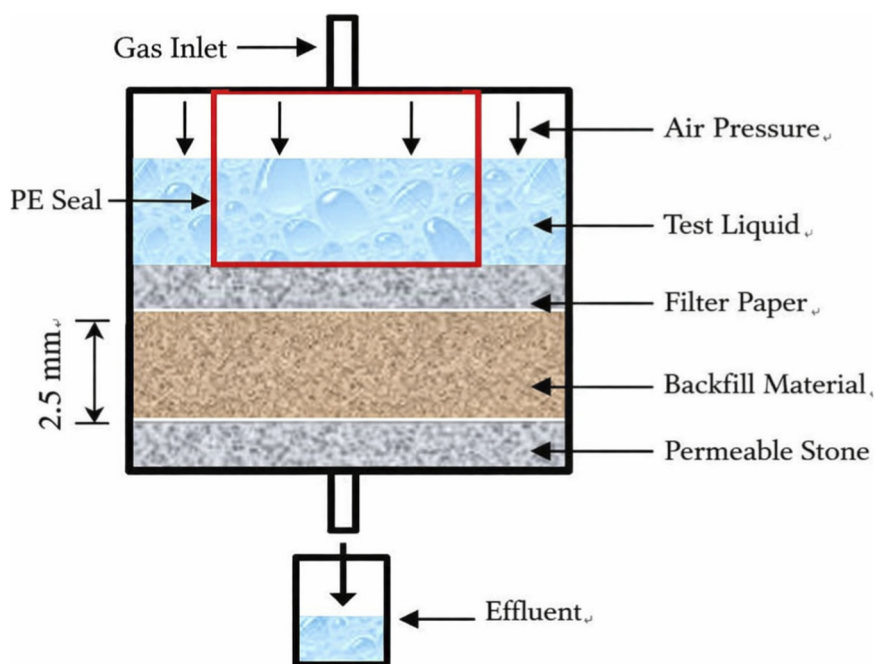


FIGURE 2
Schematic diagram of the modified filtrate loss test.

calculated based on the water content and specific gravity, assuming full saturation. The total pressure in Equation 4 was taken as the air pressure, as advised by Chung and Daniel (2008).

2.2.4 Microstructural analysis

Scanning electronic micrograph (SEM) analyses were performed on CB and XB filter cake samples to examine the microstructure of Xanthan gum-modified bentonite before and after exposure to $\text{Pb}(\text{NO}_3)_2$ solutions, using a Hitachi SU3500 Scanning Electron Microscope. The bentonite filter cakes were frozen for 5 min utilizing liquid nitrogen and subsequently transferred to a vacuum freeze-drying apparatus for a duration of 24 h at a temperature of -79°C . Following the freeze-drying process, the primary dry filter cakes were sectioned into small blocks with an approximate surface area of 0.25 cm^2 . These samples were then coated with a thin layer of gold and subjected to SEM analyses.

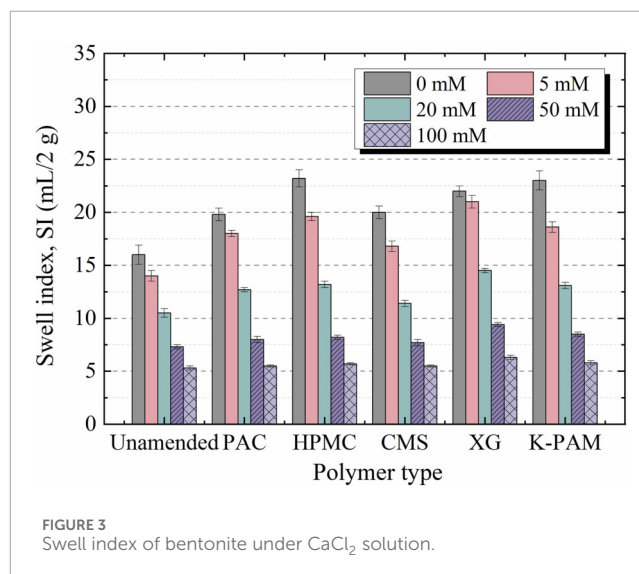


FIGURE 3
Swell index of bentonite under CaCl_2 solution.

3 Test results analysis and discussion

3.1 Polymer optimal selection results

3.1.1 Swell index

Figure 3 shows the variation in swell index (SI) of polymer-amended bentonites in CaCl_2 solutions. In deionized water (0 mM CaCl_2), all polymer amendments significantly increased SI values compared to CB. Specifically, the HPMC-amended bentonite demonstrated the most significant improvement, with SI increasing from $15.9\text{ mL}/2\text{ g}$ (unamended) to $23.2\text{ mL}/2\text{ g}$. Under CaCl_2 solutions, the SI of all polymer-amended bentonites decreased

as CaCl_2 concentration increased. At 20 mM CaCl_2 , the CMS-amended bentonite exhibited SI values similar to those of CB. By 50 mM CaCl_2 , all amended bentonites displayed SI values (around 7–10 mL/2 g) that matched CB, reflecting the typical swell behavior of calcium bentonite.

These findings align with previous research indicating that high-valence cations like Ca^{2+} decrease swell capacity by shrinking the diffuse double layer, as observed in untreated calcium bentonites. When ionic strength reaches 100 mM CaCl_2 , both amended and unamended bentonites exhibit similar SI values

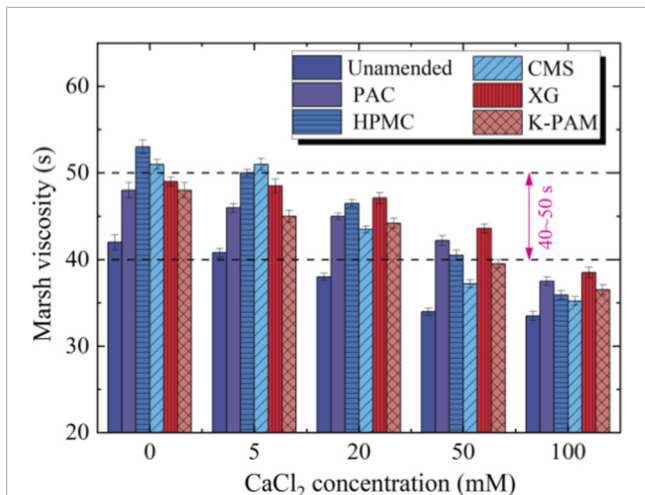


FIGURE 4 Marsh viscosity of polymer-amended bentonite slurries under CaCl₂ solutions.

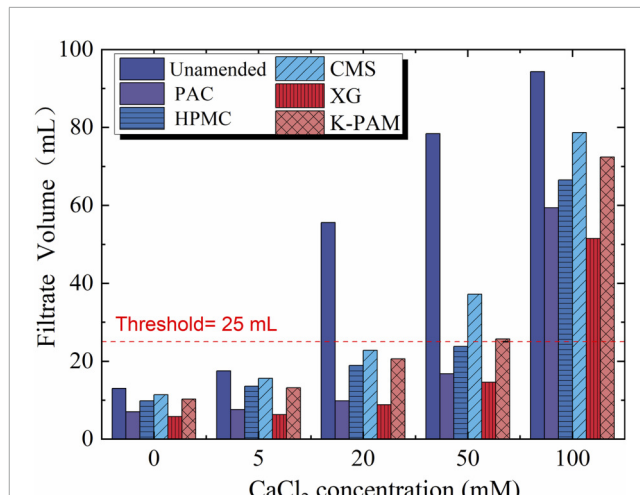


FIGURE 5 Fluid loss volume of polymer-amended bentonite slurries under CaCl₂ solutions.

of 5–6 mL/2 g, suggesting that polymer amendments are less effective under high ionic strength. Adding high-swell polymers enhances swelling in deionized water; however, increasing the CaCl₂ concentration reduces swelling for both types. The positive effect of polymers diminishes at high salt levels, with SI values ranging from 5 to 6 mL/2 g at 100 mM. This finding aligns with that of Scalia et al. (2014) and Li et al. (2025), suggesting that polymer addition does not significantly enhance seepage resistance in aggressive environments. The decreased effectiveness of polymers at high ionic strength reflects their limited ability to stabilize the structure amid strong electrostatic interactions with divalent cations.

3.1.2 Workability of bentonite slurry

Figure 4 illustrates the changes in Marsh viscosity of polymer-amended bentonite slurries under CaCl₂ solution environment. In deionized water, all polymer amendments increased the Marsh viscosity relative to unamended bentonite; HPMC-amended bentonite exhibited the highest viscosity (53 s). The viscosity values of other amended bentonites ranged between 40 and 50 s, satisfying the workability requirements for bentonite slurry. With CaCl₂ concentration increasing, Marsh viscosity decreased in both unamended and amended bentonites. At 20 mM CaCl₂, the viscosity of unamended bentonite dropped to 38 s (below the required 40–50 s threshold), whereas amended bentonites retained compliance with workability standards. At 50 mM CaCl₂ (Ca²⁺ concentration: 2000 mg/L), PAC- and XG-amended bentonite-maintained viscosities of 43.5 s and 44.6 s, respectively, still meeting workability requirements. Conversely, other amended bentonites fell below 40 s and failed compliance. These results demonstrate that polymer amendment enhances the salt resistance of bentonite slurry workability, PAC and XG amendments exhibit enhanced stability in saline environments.

Figure 5 shows how fluid loss varies in polymer-amended bentonite slurries exposed to CaCl₂ solutions. Both unamended and polymer-amended slurries show a steady increase in fluid loss as

CaCl₂ concentration rises. However, at the same concentrations, polymer-amended slurries consistently have lower fluid loss than unamended bentonite. At 20 mM CaCl₂, unamended bentonite exhibited excessive fluid loss (58 mL), well above the engineering workability threshold (<25 mL), while all polymer-amended slurries kept fluid loss below 25 mL, meeting operational standards. At 50 mM CaCl₂, only PAC- and XG-amended slurries remained within limits, with fluid losses of 16.8 mL and 14.6 mL, respectively. By 100 mM CaCl₂, all slurries (amended and unamended) showed significant fluid loss (>50 mL), with XG-amended bentonite having the lowest value (still over 50 mL). Mud-water separation occurred within 3–5 min after mixing, consistent with the sedimentation behavior reported by Yang et al. (2020). This indicates that all bentonite slurries lose workability at this concentration, showing the limits of polymer amendments in reducing fluid loss under high ionic strength conditions.

3.1.3 Hydraulic performance of bentonite filter cake

Figure 6 presents the hydraulic conductivity of filter cakes from polymer-amended bentonite slurries exposed to CaCl₂ solutions. Both amended and unamended bentonite slurries are influenced by Ca²⁺ to different extents, as evidenced by their inability to form stable filter cakes above certain CaCl₂ concentrations, along with a significant increase in fluid loss and visible mud-water separation after slurry standing. The hydraulic conductivity of filter cakes from both unamended and amended bentonites rises with increasing CaCl₂ concentration. However, polymer-amended bentonites exhibit one order of magnitude lower hydraulic conductivity than unamended bentonite. At the same concentrations, PAC- and XG-amended bentonites have the lowest conductivity values among all amendments, consistent with their superior fluid loss performance observed in previous tests. Unamended bentonite fails to form a filter cake at CaCl₂ concentrations above 5 mM, whereas polymer-amended counterparts maintain structural integrity until concentrations exceed 50 mM. This indicates that polymer

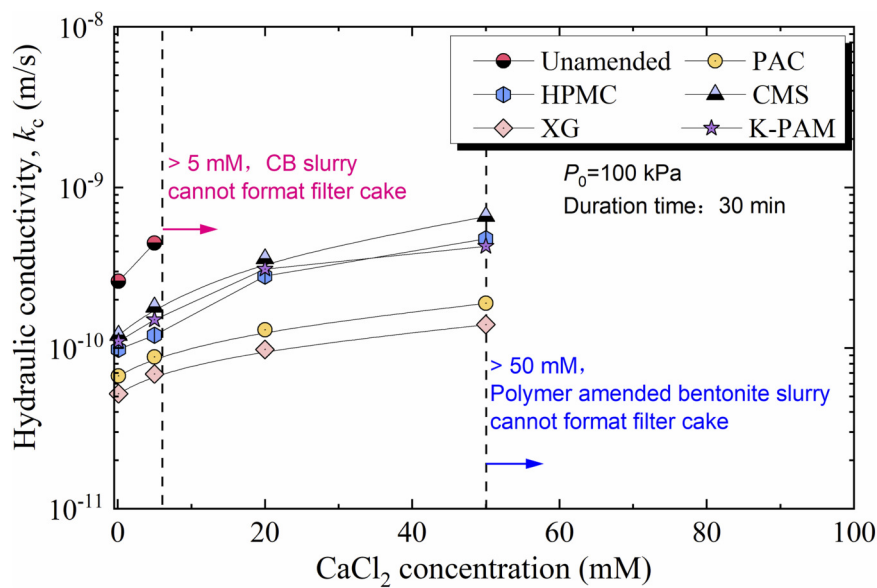


FIGURE 6
Hydraulic conductivity of polymer-amended bentonite cake under CaCl_2 solutions.

amendment greatly enhances resistance to saline erosion and prevents structural collapse.

3.1.4 Optimal polymer selection

Through a comprehensive evaluation of swell index, workability (i.e., fluid loss), and hydraulic performance of bentonite slurry, the optimal polymer was selected for subsequent investigation; the test results are summarized in Table 5. Herein, c_{\max} is defined as the threshold concentration of CaCl_2 solutions at which polymer-amended bentonite maintains workability criteria (Marsh viscosity ≥ 40 s; fluid loss ≤ 25 mL). A higher c_{\max} value signifies superior chemical compatibility of the amended bentonite. For instance, PAC-amended bentonite achieved acceptable Marsh viscosity (42.2 s) at 50 mM CaCl_2 but failed at 100 mM (37.5 s), resulting in $c_{\max} = 50$ mM. Although polymer amendment increased the swell index in deionized water, it considerably decreased swelling in CaCl_2 solutions. This demonstrates the limited effectiveness of polymers in enhancing salt-affected swell performance. As a result, swell behavior was excluded from polymer screening criteria, with a focus on workability and impermeability metrics.

A comparative analysis of the c_{\max} values shows that PAC-, HPMC-, and XG-amended bentonites have better workability retention in saline environments. In 50 mM CaCl_2 , these three polymer-enhanced bentonites keep Marsh viscosity at or above 40 s and fluid loss at or below 25 mL, fully meeting construction standards; their fluid loss volumes were 16.8 mL, 23.8 mL, and 14.6 mL, respectively, with filter cake hydraulic conductivities (k_c) of 1.9×10^{-10} m/s, 4.8×10^{-10} m/s, and 1.4×10^{-10} m/s. Other tested polymers, however, failed to meet these thresholds under the same salinity conditions.

The findings demonstrate that PAC-, HPMC-, and XG-amended bentonites effectively contribute to fluid loss control and permeability reduction, as evidenced by the minimal fluid

loss and hydraulic conductivity observed under identical ionic conditions. Among these polymer-modified bentonites, the XG-enhanced variant displays the lowest fluid loss and hydraulic conductivity. Consequently, xanthan gum (XG) has been identified as the most suitable additive for subsequent research into the anti-seepage and contaminant containment capabilities of polymer-enhanced bentonite barrier systems. Henceforth, XG-enhanced bentonites shall be referred to as XB.

3.2 Engineering property of polymer-amended bentonite

3.2.1 Basic characteristic of polymer-amended bentonite

The variation in specific gravity, swell index, and liquid limit of XB with varying polymer dosage is summarized in Table 6. The specific gravity (G_s) of XB exhibits an inverse relationship with polymer dosage. Within the 0%–4% dosage range, G_s decreased from 2.72 to 2.66. This pattern is consistent with the literature, which documents lower G_s in polymer-amended sodium bentonites. Guler et al. (2018) reported G_s of polymer-amended soils as similar to or lower than untreated soil; Scalia and Benson (2017) also recorded a G_s of 2.67 for BPN polymer-amended bentonite compared to 2.71 for unamended soil ($G_s = 2.71$). The observed G_s reduction is attributed to the intrinsic low density of superabsorbent polymers (1.24 for XG), analogous to sodium carboxymethyl cellulose, propylene carbonate, and polyacrylate (Bohnhoff and Shackelford, 2014). These polymers expand interlayer spacing and generate a more porous fabric, which is consistent with their significantly lower density (1.26–1.24 g/cm³) compared to bentonite ($G_s = 2.72$). Consequently, increased polymer dosage correlates with progressively declining in amended bentonites.

TABLE 5 Swell index, fluid loss volume, and hydraulic performance of bentonite slurry.

Parameters	Polymer-amended bentonite					
	CB	PAC	HPMC	CMS	XG	K-PAM
SI _w (mL/2 g)	15.9	20	23.2	24.1	22.2	23
k _w (m/s)	1.2 × 10 ⁻⁹	6.7 × 10 ⁻¹¹	9.8 × 10 ⁻¹¹	1.2 × 10 ⁻¹⁰	5.7 × 10 ⁻¹¹	1.1 × 10 ⁻¹⁰
c _{max} (mM)	5	50	50	20	50	20
SI _c (mL/2 g), at 50 mM CaCl ₂	7.3	8	8.2	7.7	9.4	8.5
V (mL), at 50 mM CaCl ₂	—	16.8	23.8	37.2	14.6	25.7
k _c (m/s), at 50 mM CaCl ₂	—	1.9 × 10 ⁻¹⁰	4.8 × 10 ⁻¹⁰	6.6 × 10 ⁻¹⁰	1.4 × 10 ⁻¹⁰	4.3 × 10 ⁻¹⁰

TABLE 6 Variation of specific gravity, swell index, and liquid limit of XB with polymer dosages.

Parameters	Xanthan gum dosage in bentonite (%)				
	0	0.5	1	2	4
Specific gravity, G _s	2.72	2.71	2.70	2.68	2.66
Swell index, SI (mL/2 g)	15.9	17.9	20.1	22.0	24.2
Liquid limit, w _L (%)	269	304	341	375	403

TABLE 7 Workability value of bentonite slurry with various dosages.

Parameters	Target value	Mass ratio of bentonite in slurry		
		6%	8%	10%
Filtrate volume (mL)	≤25	22.5	16.5	10.5
Marsh viscosity (s)	40–45	36	40.2	43
Density (g/cm ³)	1.05–1.10	1.036	1.047	1.058
pH	6.5–10.0	9.12	9.22	9.31

The SI of XG shows a positive correlation with polymer dosage. The unamended bentonite (CB) recorded an SI of 15.9 mL/2 g, while XB with 4% dosage achieved an SI of 24.2 mL/2 g. These values fall within the typical SI range (20–30 mL/2 g) of sodium bentonites. The liquid Limit (w_L) variations for both amended bentonites show that w_L increases proportionally with polymer dosage. CB exhibited a w_L of 267%, while XB, with a 4% dosage, reached a w_L of 403%, indicating exponential growth compared to CB. The improved swelling behavior and liquid limits were attributed to the numerous hydrophilic functional groups (such as carboxylate, COO⁻, and hydroxyl, -OH) present in Xanthan gum. These groups provide the material with excellent water-absorbing capacity, which enhances the swell index of polymer-amended bentonites.

3.2.2 Workability of polymer-amended bentonite slurry

Table 7 delineates the workability indices of unamended bentonite slurries at various dosages. The results indicate that slurries with bentonite dosages exceeding 8% satisfy the construction standards. To evaluate the efficacy of polymer amendments on bentonite, a slurry with suboptimal workability (specifically a 6% dosage) was selected for experimental analysis.

Figure 7 shows the workability indices of XB slurries with xanthan gum (XG) content from 0% to 4%. As the XG dosage increases, the filtration loss, pH, and slurry density decrease,

while the Marsh funnel viscosity increases. At a critical XG dosage of 2%, the slurry has a filtration loss of 12.5 mL, Marsh viscosity of 42.5 s, pH of 9.03, and density of 1.032 g/cm³, meeting all the specified requirements for construction workability. The results indicate that XB slurry significantly improves: (1) trench wall stabilization to prevent collapse in isolation walls; (2) pumping efficiency and cuttings suspension capacity; (3) the anti-flocculation performance of bentonite; and (4) formation pressure equilibrium to reduce fluid loss. Although pH was not independently controlled in this study, the measured pH differences between CaCl₂ and Pb(NO₃)₂ solutions provide insight into their distinct impacts on ionic transport behavior. CaCl₂ solutions exhibited near-neutral pH values, whereas Pb(NO₃)₂ solutions were moderately acidic. The lower pH in Pb(NO₃)₂ solutions increases H⁺ concentration, which suppresses the ionization of functional groups on xanthan gum molecular chains and weakens polymer-cation complexation. As a result, a higher proportion of free Pb²⁺ ions participates in cation exchange within bentonite interlayers, leading to stronger compression of the diffuse double layer, enhanced particle flocculation, and increased permeability. In contrast, the near-neutral pH environment of CaCl₂ solutions favors polymer hydration and pore-sealing effects, thereby reducing ionic transport and maintaining lower hydraulic conductivity. These results indicate that pH indirectly influences ion solubility and transport by regulating polymer conformation and cation exchange processes in polymer-amended bentonite systems.

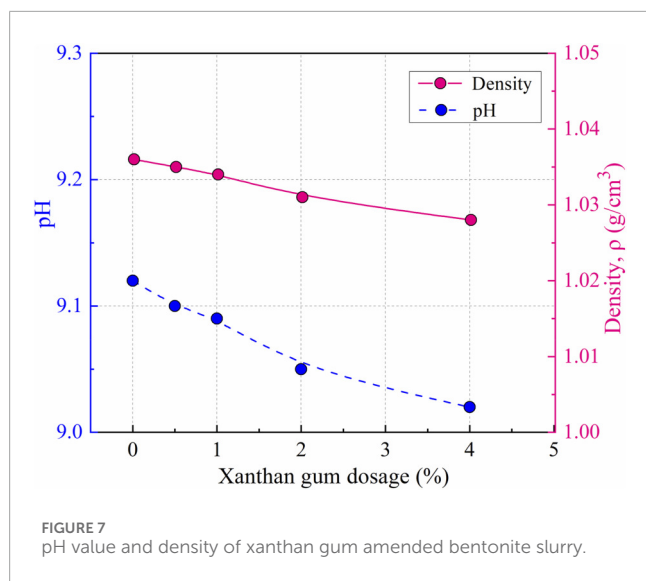


FIGURE 7
pH value and density of xanthan gum amended bentonite slurry.

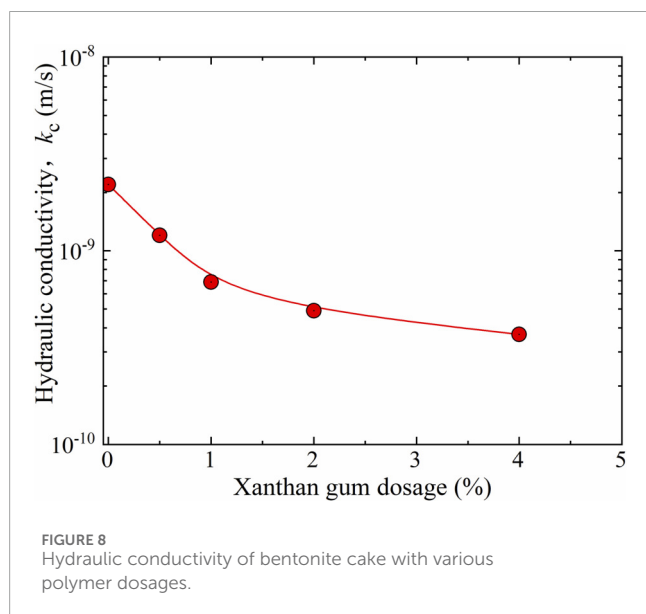


FIGURE 8
Hydraulic conductivity of bentonite cake with various polymer dosages.

3.2.3 Hydraulic performance of polymer-amended bentonite slurry

Figure 8 illustrates the curve of filter cake hydraulic conductivity versus xanthan gum (XG) dosage. The results indicate that the hydraulic conductivity of bentonite filter cakes steadily decreases as the polymer content increases. The filter cake from unamended bentonite slurry (6% dosage) has a hydraulic conductivity of 1.5×10^{-9} m/s; in contrast, adding 4% XG reduces this value to 3.7×10^{-10} m/s for the amended slurry. This represents a nearly order-of-magnitude reduction compared to the unamended system, confirming that XG amendment effectively reduces permeability in bentonite filter cakes. However, more research is needed to understand its permeability behavior when exposed to contaminated leachate and the microscopic mechanisms involved (Lee et al., 2016).

3.3 Chemical compatibility of polymer-amended bentonite

3.3.1 Chemical compatibility of bentonite with CaCl_2 solution

3.3.1.1 Filtrate loss volume and filter cake thickness

Figure 9a illustrates the relationship between filtrate loss volume and CaCl_2 solution concentration. Overall, the filtrate loss volume of all specimens increases progressively with rising CaCl_2 concentration. Notably, the unamended bentonite (CB) exhibits significantly higher sensitivity to variations in concentration, especially under 15 mM CaCl_2 solution, where the filtrate loss of CB exceeds 25 mL, thus violating slurry workability criteria. Conversely, the xanthan gum-amended bentonite (XB) maintains filtrate loss below 25 mL, similar to its performance in deionized water. However, at concentrations exceeding 60 mM, XB experiences catastrophic degradation, with filtrate loss increasing to between 70 and 120 mL, a measurement that was hindered by cylinder overflow.

Figure 9b illustrates the relationship between filter cake thickness and CaCl_2 concentration. Both specimens exhibit an increase in thickness corresponding to rising concentration; however, CB consistently produces thicker cakes than XB. The thickness of CB nearly doubles, from 2–2.5 mm to 4–5 mm, as the concentration increases from 0 to 15 mM, whereas the thickness of XB remains relatively stable. At a concentration of 60 mM, the thickness of XB increases to approximately 3–3.5 mm, demonstrating a significant sensitivity to saline concentration.

The observed trends in filtrate loss and filter cake thickness primarily result from the following mechanism: Higher calcium chloride concentrations increase the displacement of exchangeable cations within bentonite interlayers, leading to compression of the electric double layer. This compression weakens colloidal repulsive forces, leading to particle aggregation and flocculation (Pan et al., 2024; Min et al., 2019). As a result, these flocculated structures quickly settle on the surface of the filter paper, ultimately worsening both filtrate loss volume and cake thickness.

3.3.1.2 Hydraulic conductivity, swell index, and filtrate loss volume

Figure 10 shows the relationship between the hydraulic conductivity of the XB filter cake, swell index, and filtrate loss volume. The results indicate that as the filtrate loss volume increases, the hydraulic conductivity of the filter cake also rises. Under the same conditions, the hydraulic conductivity of unamended bentonite (CB) filter cake is about ten times higher than that of xanthan gum-amended bentonite (XB) filter cake. Regarding the relationship between filter cake permeability and bentonite swell index, a decrease in swell index corresponds to a gradual increase in hydraulic conductivity; this growth trend becomes more pronounced at lower swell indices. Compared to unamended CB, the hydraulic conductivity of XB filter cake demonstrates less sensitivity to changes in swell index. Specifically, when the swell index decreases from 16 mL/2 g to 10 mL/2 g, the hydraulic conductivity of CB filter cake increases by approximately one order of magnitude, whereas that of XB filter cake rises by no more than four times.

It appears that the permeability of polymer-amended bentonite is influenced not only by variations in the swell index, which reflects cation exchange effects, but also by the physical impact of polymer

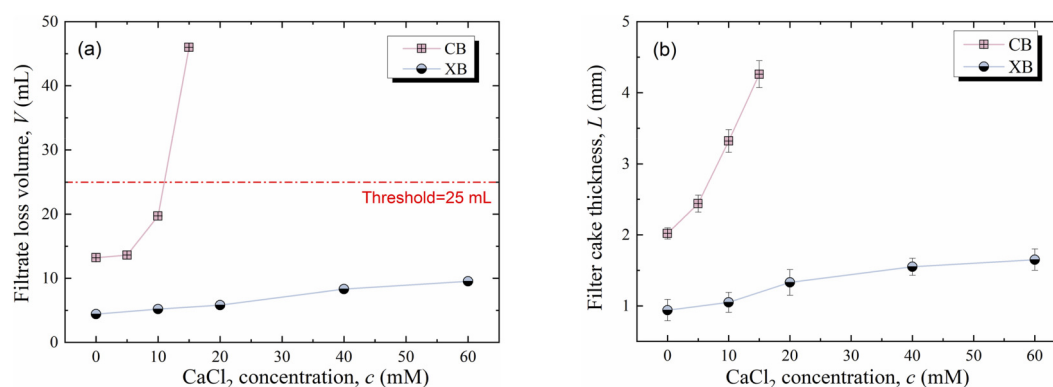


FIGURE 9 Relationships between filtrate loss volume (V), filter cake thickness (L), and CaCl_2 concentration (c): (a) V versus c ; and (b) L versus c .

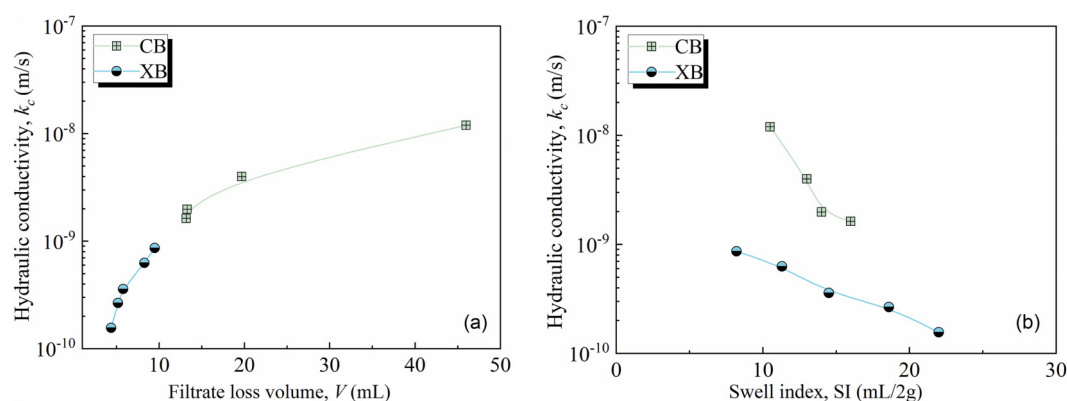


FIGURE 10 Relationship between hydraulic conductivity (k_c), Filtrate loss volume (V), and Swell index (SI): (a) k_c versus V ; and (b) k_c versus SI .

additives. Regarding swelling mechanisms, cation exchange within bentonite interlayers in CaCl_2 solutions compresses the electric double layer (EDL), resulting in a reduced swell index and expanded flow channels, thereby enhancing permeability. Although cation exchange and decreased swelling continue to occur in salt solutions following polymer modification, the polymers physically seal the gaps between bentonite particles, constricting flow channels and increasing the complexity of the flow path.

3.3.2 Variation in chemical compatibility of bentonite exposed to lead and calcium solutions

To examine the effect of cation species on the chemical compatibility of bentonite, this section compares the filtrate test results when exposed to lead nitrate ($\text{Pb}(\text{NO}_3)_2$) and calcium chloride (CaCl_2). Equal contaminant concentrations and test pressure ($P_0 = 100$ kPa) were used to evaluate the impacts of Pb^{2+} and Ca^{2+} ions on filtrate loss volume, filter cake thickness, and permeability properties.

3.3.2.1 Differences in filtrate loss and cake thickness

Figure 11 illustrates the relationship between solution concentration (c), filtrate loss volume (V), and filter cake thickness

(L) for each specimen. Results show that both filtrate loss volume and cake thickness increase with increasing solution concentration; compared to Ca^{2+} , Pb^{2+} has a more significant negative impact on the permeability and swelling properties of bentonite. At 40 mM $\text{Pb}(\text{NO}_3)_2$ concentration, the filtrate loss volume of XB approaches the slurry workability limit (<25 mL), while at 60 mM CaCl_2 concentration, XB maintains filtrate loss below 10 mL.

3.3.2.2 Difference in hydraulic performance

The hydraulic conductivity (k_c) and permeability ratio (k_c/k_w) for both filter cakes under $\text{Pb}(\text{NO}_3)_2$ and CaCl_2 solutions are presented in Figure 12. As the concentration of solutions increases, the hydraulic conductivities of both specimens generally increase. Both solutions significantly influence the permeability of the filter cake composed of unamended bentonite (CB): when the concentration rises from 0 to 15 mM, the hydraulic conductivity increases by approximately one order of magnitude. Compared to CaCl_2 solutions, $\text{Pb}(\text{NO}_3)_2$ solutions exert a more substantial effect on the permeability of the XB filter cake.

Although CaCl_2 concentrations reach 40–60 mM, the k_c/k_w of XB remains at 5.2, indicating that permeability has not

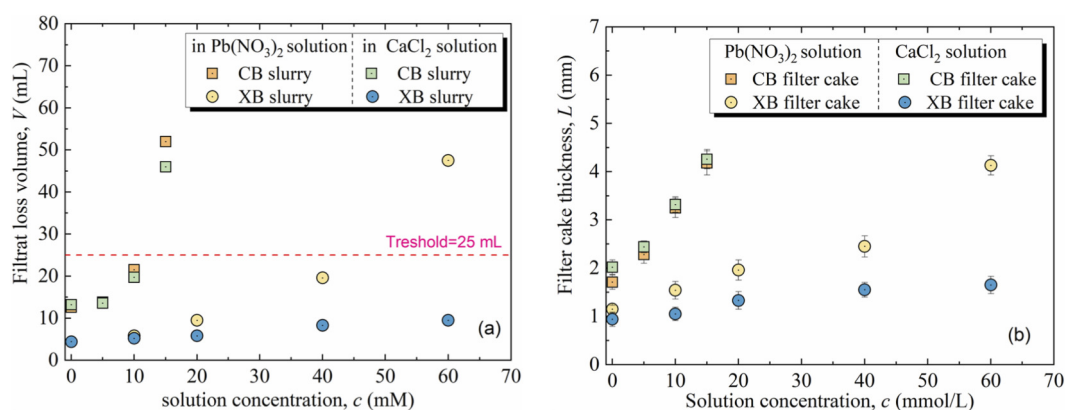


FIGURE 11 Relationship between Filtrate loss volume (V), filter cake thickness (L), and $\text{Pb}(\text{NO}_3)_2$ concentration (c): (a) V versus c ; and (b) L versus c .

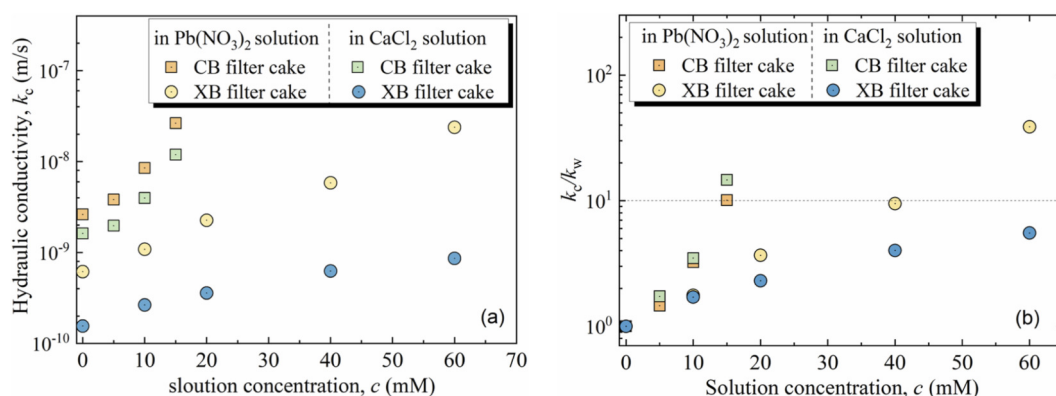


FIGURE 12 Relationship between Hydraulic conductivity (k_c) and solution concentration (c): (a) k_c versus c ; and (b) k_c/k_{cw} versus c .

significantly increased. The differing effects of Pb^{2+} and Ca^{2+} on filtrate loss, cake thickness, and amended slurry permeability are attributed to pH variations: test solutions with CaCl_2 had pH values ranging from 6.25 to 6.65, while $\text{Pb}(\text{NO}_3)_2$ solutions ranged from 4.68 to 4.97. A lower pH increases H^+ ion concentration, which inhibits the ionisation of hydroxyl (-OH) and carboxyl (-COOH) groups on xanthan gum (XG) molecular chains, preventing the formation of complexes between these functional groups and Pb^{2+} .

This increases the free Pb^{2+} concentration, promotes cation exchange in bentonite interlayers, compresses the electric double layer, and enhances particle flocculation and deposition, resulting in thicker filter cakes under $\text{Pb}(\text{NO}_3)_2$, ultimately increasing filter cake permeability.

3.4 Microstructural characteristic

The SEM results provide critical insight into the microstructural mechanisms governing the hydraulic and transport behavior of polymer-amended bentonite under different chemical

environments. As shown in Figure 13a, the unamended bentonite (CB) in deionized water exhibits a relatively uniform but loosely packed honeycomb-like fabric, which is characteristic of hydrated bentonite with limited interparticle bonding. This open structure allows the formation of continuous pore channels, explaining the comparatively higher hydraulic conductivity observed in CB filter cakes. In contrast, the xanthan gum-amended bentonite (XB) in deionized water (see Figure 13b) displays a markedly different microstructure. A three-dimensional polymer-clay network is clearly observed, where hydrated xanthan gum chains form continuous bridges between bentonite aggregates. These polymer bridges bind water molecules to form a hydrogel matrix and effectively fill and constrict intergranular pores, resulting in a denser fabric with reduced pore connectivity. This microstructural arrangement increases flow path tortuosity and significantly inhibits ionic transport, which is consistent with the lower filtrate loss and hydraulic conductivity measured for XB under neutral pH conditions. When XB is exposed to $\text{Pb}(\text{NO}_3)_2$ solution (see Figure 13c), the microstructure undergoes substantial degradation. The polymer network becomes discontinuous, and the polymer strands appear thicker and more sparsely distributed,

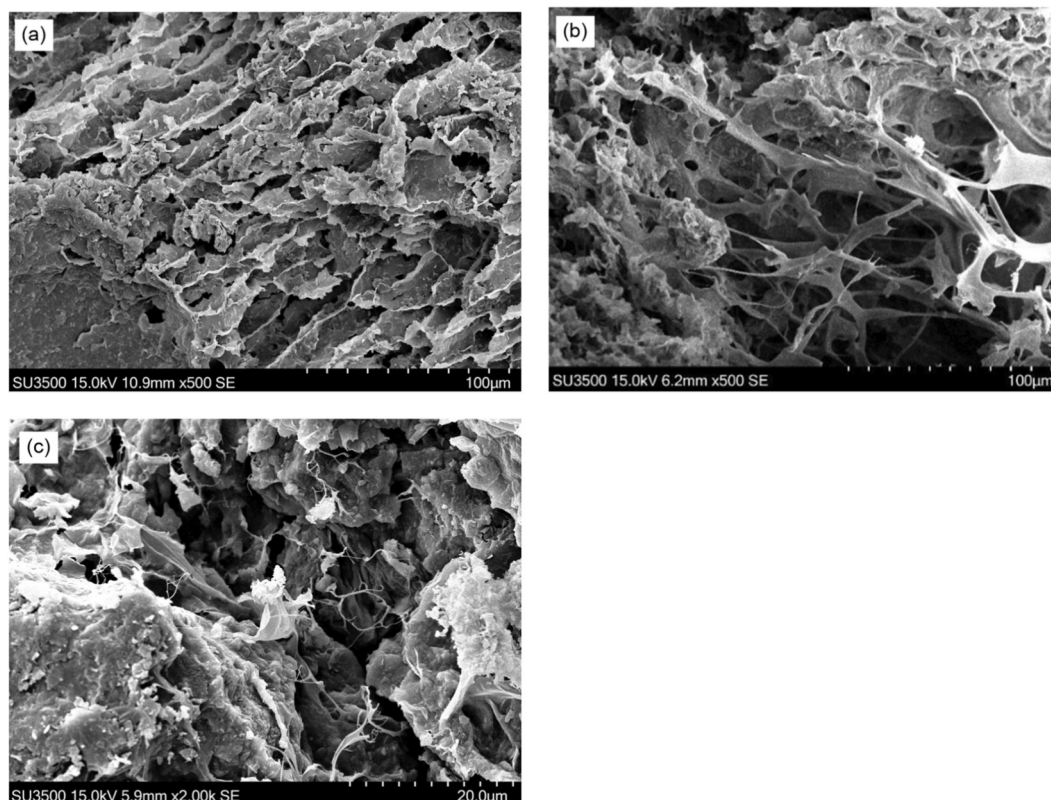


FIGURE 13 SEM images of filter cake samples for (a) CB in deionized water; (b) XB in deionized water; and (c) XB exposed to 40 mM $\text{Pb}(\text{NO}_3)_2$ solution.

accompanied by enlarged inter-aggregate pores. This change is attributed to the acidic pH of the $\text{Pb}(\text{NO}_3)_2$ solution, which suppresses the ionization of carboxyl and hydroxyl functional groups on xanthan gum molecular chains. The resulting reduction in electrostatic repulsion and polymer hydration induces a transition of polymer conformation from an extended to a coiled state, thereby weakening polymer–clay interactions and diminishing the pore-sealing capability of the hydrogel network (Shen and Wei, 2018; Tian et al., 2019). Meanwhile, the increased availability of free Pb^{2+} ions enhances cation exchange and compresses the diffuse double layer of bentonite, promoting particle flocculation and the development of preferential flow channels.

Overall, the SEM observations demonstrate that the hydraulic performance of polymer-amended bentonite is governed by the stability of the polymer–clay network, which is strongly influenced by solution chemistry and pH. Under near-neutral conditions, the extended polymer network effectively restricts pore connectivity and ionic transport, whereas under acidic conditions, polymer collapse and intensified cation exchange lead to microstructural coarsening and increased permeability (Wireko et al., 2022). These findings provide direct microstructural evidence linking pH-dependent polymer behavior to the macroscopic transport properties of bentonite filter cakes.

4 Conclusion

A series of fundamental property assessments, swelling index evaluations, and magnetic flux leakage (MFL) permeability tests were conducted to examine the effect of polymer modifications on the hydraulic conductivity of standard bentonite filter cakes used in slurry trench walls, with various concentrations of CaCl_2 solutions. The results of this research indicate the following conclusions:

1. Five selected polymer amendments substantially improve the swelling capacity and chemical stability of bentonite in saline environments. Notably, xanthan gum-modified bentonite outperformed all others in terms of swelling and hydraulic performance, making it the preferred choice for future research. As the xanthan gum dosage increases, the swell index and liquid limit of XB show an upward trend, while the specific gravity decreases. When the xanthan gum dosage reaches 4%, the permeability coefficient of the bentonite slurry filter cake drops to as low as 3.7×10^{-10} m/s, which is ten times lower than that of unmodified bentonite (1.5×10^{-9} m/s).
2. Under a 15 mM CaCl_2 solution, the filtrate loss volume of CB exceeds 25 mL, whereas the filtrate loss volume of XB is 9.5 mL when exposed to a 60 mM CaCl_2 solution. Compared to CB, the hydraulic conductivity of the XB filter cake shows less sensitivity to changes in the swell index. Specifically, when the swell index drops from 16 mL/2 g to 10 mL/2 g, the hydraulic conductivity of the CB filter cake increases by about

ten times, while that of the XB filter cake increases by no more than four times. Compared to calcium ions, lead ions have a more significant negative impact on the permeability and swelling properties of bentonite. At the same solution concentration, both CB and XB show higher filtrate loss volumes and hydraulic conductivity in $\text{Pb}(\text{NO}_3)_2$ solution than in CaCl_2 solution.

3. Polymer conformation transitions from an extended structure in deionized water to a coiled configuration in saline conditions, leading to decreased pore sealing effectiveness and increased hydraulic conductivity of XB, although it still remains lower than that of CB samples. Further research is necessary to verify the hypotheses of polymer clogging and to study the adsorption properties and membrane behavior of contaminant transport through the vertical cutoff wall backfills containing xanthan gum-amended bentonite.

Data availability statement

The original contributions presented in the study are included in the article/supplementary material, further inquiries can be directed to the corresponding author.

Author contributions

SS: Writing – original draft, Conceptualization, Writing – review and editing. WZ: Writing – review and editing. NQ: Writing – review and editing.

Funding

The author(s) declared that financial support was received for this work and/or its publication. This research was funded by

References

- Ashmawy, A. K., El-Hajji, D., Sotelo, N., and Muhammad, N. (2002). Hydraulic performance of untreated and polymer-treated bentonite in inorganic landfill leachates. *Clays Clay Minerals* 50 (5), 546–552. doi:10.1346/000986002320679288
- Balaganesh, P., Nandhini, S. S., Kumar, K. M., Ragavi, S. P., Shankar, S. A., Vasudevan, M., et al. (2023). Flow behaviour of wastewater contaminants in compost with manufactured sand (M-SAND) under layered conditions. *J. Solid Waste Technol. Manag.* 49 (3), 231–239. doi:10.5276/jswtm/ismaw/49/2/2023.231
- Bohnhoff, G. L., and Shackelford, C. D. (2014). Hydraulic conductivity of polymerized bentonite-amended backfills. *J. Geotechnical Geoenvironmental Eng.* 140 (3), 04013028. doi:10.1061/(asce)gt.1943-5606.0001034
- Chung, J., and Daniel, D. E. (2008). Modified fluid loss test as an improved measure of hydraulic conductivity for bentonite. *Geotechnical Test. J.* 31 (3), 243–251. doi:10.1520/gtj100005
- de Carvalho Balaban, R., Vidal, E. L. F., and Borges, M. R. (2015). Design of experiments to evaluate clay swelling inhibition by different combinations of organic compounds and inorganic salts for application in water base drilling fluids. *Appl. Clay Sci.* 105, 124–130. doi:10.1016/j.clay.2014.12.029
- Di Emidio, G., Mazzieri, F., Verastegui-Flores, R. D., Van Impe, W., and Bezuijen, A. (2015). Polymer-treated bentonite clay for chemical-resistant geosynthetic clay liners. *Geosynth. Int.* 22 (1), 125–137. doi:10.1680/gein.14.00036
- Di Maio, C. (1996). Exposure of bentonite to salt solution: osmotic and mechanical effects. *Géotechnique* 46 (4), 695–707. doi:10.1680/geot.1996.46.4.695
- the Natural Science Foundation of the Jiangsu Higher Education Institutions of China (Grant No. 22KJB560021), the Scientific Research Fund Project of Nanjing Vocational Institute of Transport Technology (Grant No. JZ2206), and the Research Initiation Program for High-Level Talents at Nanjing Vocational Institute of Transport Technology (Grant No. JG2530).

Conflict of interest

The author(s) declared that this work was conducted in the absence of any commercial or financial relationships that could be construed as a potential conflict of interest.

Generative AI statement

The author(s) declared that generative AI was not used in the creation of this manuscript.

Any alternative text (alt text) provided alongside figures in this article has been generated by Frontiers with the support of artificial intelligence and reasonable efforts have been made to ensure accuracy, including review by the authors wherever possible. If you identify any issues, please contact us.

Publisher's note

All claims expressed in this article are solely those of the authors and do not necessarily represent those of their affiliated organizations, or those of the publisher, the editors and the reviewers. Any product that may be evaluated in this article, or claim that may be made by its manufacturer, is not guaranteed or endorsed by the publisher.

- Li, Y. C., Cleall, P. J., Wen, Y. D., Chen, Y. M., and Pan, Q. (2015). Stresses in soil-bentonite slurry trench cut-off walls. *Geotechnique* 65 (10), 843–850. doi:10.1680/geot.14.p.219
- Li, Y. C., Chen, G. N., Chen, Y. M., and Cleall, P. J. (2017). Design charts for contaminant transport through slurry trench cutoff walls. *J. Environ. Eng.* 143 (9), 06017005. doi:10.1061/(asce)ee.1943-7870.0001253
- Li, Q., Jia, Z., and Zhao, Y. (2021a). Laboratory evaluation of hydraulic conductivity and chemical compatibility of bentonite slurry for grouting walls. *Environ. Earth Sci.* 80 (17), 569. doi:10.1007/s12665-021-09847-5
- Li, Q., Chen, J., Benson, C. H., and Peng, D. (2021b). Hydraulic conductivity of bentonite-polymer composite geosynthetic clay liners permeated with bauxite liquor. *Geotext. Geomembranes* 49 (2), 420–429. doi:10.1016/j.geotexmem.2020.10.015
- Li, D., Jiang, Z., Tian, K., and Ji, R. (2025). Estimation of the hydraulic conductivity of bentonite-polymer GCLs with machine learning techniques. *Environ. Geotech.* 12 (6), 433–451. doi:10.1680/jenge.24.00002
- Liu, Y., Gates, W. P., Bouazza, A., and Rowe, R. K. (2014). Fluid loss as a quick method to evaluate hydraulic conductivity of geosynthetic clay liners under acidic conditions. *Can. Geotechnical J.* 51 (2), 158–163. doi:10.1139/cgj-2013-0241
- Liu, S. Y., Fan, R. D., Du, Y. J., and Yang, Y. L. (2016). Modified fluid loss test to measure the hydraulic conductivity of heavy metal-contaminated bentonite filter cakes. *Geo-Chicago 2016*, 568–577.
- Malusis, M. A., and McKeehan, M. D. (2013). Chemical compatibility of model soil-bentonite backfill containing mult swellable bentonite. *J. Geotechnical Geoenvironmental Eng.* 139 (2), 189–198. doi:10.1061/(asce)gt.1943-5606.0000729
- Masoodhu, S. S., Natarajan, N., and Vasudevan, M. (2025). Hydraulic conductivity performance of polymer-modified composite GCLs subjected to inorganic salt solutions. *J. Mater. Eng. Perform.*, 1–19. doi:10.1007/s11665-025-12906-8
- Mazzieri, F., Di Emidio, G., and Pasqualini, E. (2017). Effect of wet-and-dry ageing in seawater on the swelling properties and hydraulic conductivity of two amended bentonites. *Appl. Clay Sci.* 142, 40–51. doi:10.1016/j.clay.2016.10.031
- Min, F., Du, J., Zhang, N., Chen, X., Lv, H., Liu, L., et al. (2019). Experimental study on property change of slurry and filter cake of slurry shield under seawater intrusion. *Tunn. Undergr. Space Technol.* 88, 290–299. doi:10.1016/j.tust.2019.03.006
- Opdyke, S. M., and Evans, J. C. (2005). Slag-cement-bentonite slurry walls. *J. Geotechnical Geoenvironmental Eng.* 131 (6), 673–681. doi:10.1061/(asce)1090-0241(2005)131:6(673)
- Pan, Z., Ou-yang, L., Shao, Y., Li, Y., and Sun, L. (2024). Performance and deterioration mechanisms of PAC amended calcium bentonite in seawater with different compositions. *Case Stud. Constr. Mater.* 20, 02869. doi:10.1016/j.cscm.2024.e02869
- Pandey, M. R., Badiger, S., and Sivakumar Babu, G. L. (2019). Effects of bentonite and polymer soil amendment on contaminant transport parameters. *J. Hazard. Toxic, Radioact. Waste* 23 (1), 04018034. doi:10.1061/(asce)hz.2153-5515.0000427
- Philip, L. K. (2001). An investigation into contaminant transport processes through single-phase cement-bentonite slurry walls. *Eng. Geology* 60 (1-4), 209–221. doi:10.1016/s0013-7952(00)00102-2
- Rout, S., and Singh, S. P. (2020). Effect of inorganic salt solutions on physical and mechanical properties of bentonite based liner. *J. Hazard. Toxic, Radioact. Waste* 24 (4), 04020053. doi:10.1061/(asce)hz.2153-5515.0000553
- Ryan, C., Ruffing, D., and Evans, J. C. (2022). "Soil bentonite slurry trench cutoff walls: history, design, and construction practices," in *Geo-congress 2022*, 89–99.
- Scalia, J., and Benson, C. H. (2017). Polymer fouling and hydraulic conductivity of mixtures of sodium bentonite and a bentonite-polymer composite. *J. Geotechnical Geoenvironmental Eng.* 143 (4), 04016112. doi:10.1061/(asce)gt.1943-5606.0001628
- Scalia, J., Benson, C. H., Bohnhoff, G. L., Edil, T. B., and Shackelford, C. D. (2014). Long-term hydraulic conductivity of a bentonite-polymer composite permeated with aggressive inorganic solutions. *J. Geotechnical Geoenvironmental Eng.* 140 (3), 04013025. doi:10.1061/(asce)gt.1943-5606.0001040
- Setz, M. C., Tian, K., Benson, C. H., and Bradshaw, S. L. (2017). Effect of ammonium on the hydraulic conductivity of geosynthetic clay liners. *Geotext. Geomembranes* 45 (6), 665–673. doi:10.1016/j.geotexmem.2017.08.008
- Sharma, H. D., and Reddy, K. R. (2004). *Geoenvironmental engineering: site remediation, waste containment, and emerging waste management technologies*. Hoboken, NJ: John Wiley & Sons, Inc.
- Shen, S. Q., and Wei, M. L. (2018). Hydraulic conductivity of polymer-amended sand-bentonite backfills permeated with lead nitrate solutions. *Adv. Civ. Eng.* 1, 9435194. doi:10.1155/2018/9435194
- Syed Masoodhu, S., Natarajan, N., and Vasudevan, M. (2024). Modification of bentonite with black cotton soil and carboxyl methyl cellulose for the enhancement of hydraulic performance of geosynthetic clay liners. *Water Sci. & Technol.* 89 (7), 1846–1859. doi:10.2166/wst.2024.093
- Tian, K., Likos, W. J., and Benson, C. H. (2019). Polymer elution and hydraulic conductivity of bentonite-polymer composite geosynthetic clay liners. *J. Geotechnical Geoenvironmental Eng.* 145 (10), 04019071. doi:10.1061/(asce)gt.1943-5606.0002097
- Tong, S., Wei, L. L., Evans, J. C., Chen, Y. M., and Li, Y. C. (2022). Numerical analysis of consolidation behavior of soil-bentonite backfill in a full-scale slurry trench cutoff wall test. *Soils Found.* 62 (5), 101188. doi:10.1016/j.sandf.2022.101188
- Wireko, C., Abichou, T., Tian, K., Zainab, B., and Zhang, Z. (2022). Effect of incineration ash leachates on the hydraulic conductivity of bentonite-polymer composite geosynthetic clay liners. *Waste Manag.* 139, 25–38. doi:10.1016/j.wasman.2021.12.011
- Wu, H. L., Du, Y. J., Yu, J., Yang, Y. L., and Li, V. C. (2020). Hydraulic conductivity and self-healing performance of engineered cementitious composites exposed to acid mine drainage. *Sci. Total Environ.* 716, 137095. doi:10.1016/j.scitotenv.2020.137095
- Yang, Y. L., Reddy, K. R., Zhang, W. J., Fan, R. D., and Du, Y. J. (2020). SHMP-amended Ca-bentonite/sand backfill barrier for containment of lead contamination in groundwater. *Int. J. Environ. Res. Public Health* 17 (1), 370.